Geophys. J. Int. (2008) **174,** 1138–1152 doi: 10.1111/j.1365-246X.2008.03877.x

Capturing magma intrusion and faulting processes during continental rupture: seismicity of the Dabbahu (Afar) rift

C. J. Ebinger,[1,2] D. Keir,[2,3] A. Ayele,[4] E. Calais,[5] T. J. Wright,[3] M. Belachew,[1,4] J. O. S. Hammond,[6] E. Campbell[1] and W. R. Buck[7]

[1]*Department of Earth and Environmental Sciences, University of Rochester, Rochester,* NY 14627*, USA. E-mail: ebinger@earth.rochester.edu*
[2]*Department of Geology, Royal Holloway University of London, Egham,* TW20 0EX*, UK*
[3]*School of Earth and Environmental Sciences, University of Leeds, Leeds* LS2 9JT*, UK*
[4]*Geophysical Observatory, Addis Ababa University, PO Box 1176 Addis Ababa, Ethiopia*
[5]*Department of Earth and Atmospheric Sciences, Purdue University, W Lafayette, IN, USA*
[6]*Department of Earth Sciences, University of Bristol,* BS8 1RJ*, UK*
[7]*Lamont-Doherty Earth Observatory, Palisades, NY, USA*

Accepted 2008 June 5. Received 2008 June 4; in original form 2008 January 29

SUMMARY

Continental rupture models emphasize the role of faults in extensional strain accommodation; extension by dyke intrusion is commonly overlooked. A major rifting episode that began in 2005 September in the Afar depression of Ethiopia provides an opportunity to examine strain accommodation in a zone of incipient plate rupture. Earthquakes recorded on a temporary seismic array (2005 October to 2006 April), direct observation of fault patterns and geodetic data document ongoing strain and continued dyke intrusion along the ∼60-km long Dabbahu rift segment defined in earlier remote sensing studies. Epicentral locations lie along a ∼3 km wide, ∼50 km long swath that curves into the SE flank of Dabbahu volcano; a second strand continues to the north toward Gab'ho volcano. Considering the ∼8 m of opening in the September crisis, we interpret the depth distribution of microseismicity as the dyke intrusion zone; the dykes rise from ∼10 km to the near-surface along the ∼60-km long length of the tectono-magmatic segment. Focal mechanisms indicate slip along NNW-striking normal faults, perpendicular to the Arabia–Nubia plate opening vector. The seismicity, InSAR, continuous GPS and structural patterns all suggest that magma injection from lower or subcrustal magma reservoirs continued at least 3 months after the main episode. Persistent earthquake swarms at two sites on Dabbahu volcano coincide with areas of deformation identified in the InSAR data: (1) an elliptical, northwestward-dipping zone of seismicity and subsidence interpreted as a magma conduit, and (2) a more diffuse, 8-km radius zone of shallow seismicity (<2 km) above a shadow zone, interpreted as a magma chamber between 2.5 and 6 km subsurface. InSAR and continuous GPS data show uplift above a shallow source in zone (2) and uplift above the largely aseismic Gab'ho volcano. The patterns of seismicity provide a 3-D perspective of magma feeding systems maintaining the along-axis segmentation of this incipient seafloor spreading segment.

Key words: Seismic cycle; Seismicity and tectonics; Volcano seismology; Neotectonics; Africa.

INTRODUCTION

Dyke intrusions achieve crustal accretion at divergent plate boundaries, and dykes contribute to crustal extension in some continental rift zones. The sheeted dyke complexes comprising oceanic crustal layer 2B record their passage and demonstrate that dyke intrusion efficiently accommodates most of the plate separation at seafloor spreading centres (e.g. Delaney *et al.* 1998; Macdonald 1998). Within rifts transitional between continental and oceanic, dykes may accommodate an equal or possibly larger proportion of strain than is accommodated by normal faults (e.g. Ebinger & Casey 2001; Keir *et al.* 2006a; Rowland *et al.* 2007). Yet, the process of dyke intrusion remains poorly understood because the magma rarely reaches the surface, and surface deformation is convolved with faulting triggered by the dyke intrusion (e.g. Rubin & Pollard 1988; Rubin 1992).

Dyking events result in an instantaneous and localized extension marked by intense swarms of shallow, commonly small magnitude,

and sometimes long period earthquakes, with or without effusive volcanism (e.g. Einarsson & Brandsdottir 1980; Rubin & Gillard 1998; Rubin *et al.* 1998). Migrating earthquake swarms and harmonic tremor recorded on seismic arrays, and satellite geodetic techniques allow us to map the vertical and lateral migration of magma during tectono-magmatic episodes, as well as the transient response of the plate to the stresses induced by the dyke intrusion itself. Mid-ocean ridge dyking events may occur singly or comprise a succession of discrete dyke intrusions over several years; dyke intrusions occurred over a 9-yr period in the Krafla, Iceland rift segment (e.g. Sigmundsson 2006).

Rubin *et al.* (1998) simulate the stress field surrounding a fluid filled crack, and conclude that seismicity accompanies dyke intrusion when ambient stress levels are near failure. The dyke intrusion itself may be aseismic. Buck *et al.* (2007) consider a closed magma-chamber and dyke system, and they find that dyke propagation direction and distance depend on both the pre-dyke level of stress and the thickness of the lithosphere the dyke cuts. Dykes emanating from shallow reservoirs will solidify over the time periods of propagation (e.g. Fialko & Rubin 1998), but dykes rising from greater depths and higher temperatures may cool over periods of weeks to months, effectively maintaining an open conduit at depth (Buck *et al.* 2007).

In 2005 September a tectono-magmatic event of unprecedented scale and intensity occurred along a previously identified segment of the southern Red Sea rift in northern Ethiopia (Fig. 1). The brief event consisted of an ∼60 km-long dyke intrusion signalled by 163 $5.5 > m_b > 3.9$ earthquakes between September 4 and October 4 (NEIC); models of InSAR data suggest 2.5 km^3 of magma were emplaced during the month-long episode (Wright *et al.* 2006; Ayele *et al.* 2007a,b; see Fig. 1). The number of teleseisms was more than 3 times the number recorded during the 1978 Krafla event (Einarsson & Brandsdottir 1980; Wright *et al.* 2006).

The 2005 Afar seismo-volcanic crisis provides an opportunity to study the response of a stretched continental plate to the rapid emplacement of a large magma volume. The rapid geodetic, seismic and volcanological response initiated by colleagues at Addis Ababa University ensured a nearly continuous record of events from onset of the cycle, providing new insights into a rarely observed process (Yirgu *et al.* 2006; Ayele *et al.* 2007a,b). Although the event occurred in a region with few permanent settlements and no two-story structure, the scale and duration of deformation are sobering and require re-evaluation of rift-related hazards.

This paper reports seismicity patterns from 2005 October 19 to 2006 April 1 and a comparison with deformation patterns deduced from field observations (Rowland *et al.* 2007) and InSAR data over the same time period. Our aim is to map spatial and temporal variations in the distribution of seismicity and its relation to intrusive and extrusive volcanism, fault kinematics and melt migration during the first 6 months after the Dabbahu seismo-volcanic crisis. We use these results to evaluate models for dyke intrusion and their contribution to the creation and maintenance of along-axis segmentation in rifts, at the transition from continental to oceanic rifting. These results also form a baseline for ongoing hazard mitigation efforts in Afar.

TECTONIC SETTING

Rifting of Africa and Arabia during the past ∼30 Myr produced the ∼300-km wide Afar depression, which comprises the Afar triple junction (Fig. 1). To the northeast, the Afar depression is bounded by the NW–SE trending Danakil horst, generally considered to be a rigid block rotating counter-clockwise as the Afar rift opens (e.g. Souriot & Brun 1992; Eagles *et al.* 2002). The Tendaho-Goba'ad Discontinuity is a fault scarp separating the zone of sub-EW extension in the East African rift from the NE–SW opening Red Sea rift (TGD, Fig. 1).

The Red Sea, Gulf of Aden and East African rift arms formed within a Palaeogene flood basalt province associated with the Afar mantle plume (e.g. Courtillot *et al.* 1980; Yirgu *et al.* 2006). The thermal anomaly associated with the Palaeogene mantle plume persists today, as shown by low *P*- and *S*-wave upper-mantle velocities beneath the uplifted plateaux of Arabia and NE Africa (e.g. Debayle *et al.* 2001; Benoit *et al.* 2003; Bastow *et al.* 2005; Benoit *et al.* 2006).

Rifting along the southern Red Sea within the Afar depression commenced by 29 Ma, roughly coincident with the 31–29 Ma flood basalt sequences in the same area (Wolfenden *et al.* 2005). Rifting has progressed to seafloor spreading along the length of the Gulf of Aden and in sectors of the Red Sea north of 14°N (e.g. Abdallah *et al.* 1979; Manighetti *et al.* 1997; d'Acremont *et al.* 2005). From earlier refraction/wide angle reflection and receiver function studies, the highly extended and intruded Afar crust is 18 km thick in its northern part and 26 km in the south; it bears strong similarities to crust beneath Iceland (e.g. Berckhemer *et al.* 1975; Dugda *et al.* 2006, 2007; Stuart *et al.* 2006).

Since ∼3 Ma, faulting and volcanism within the Afar depression have localized to ∼60-km long, 10-km wide zones of aligned chains of fissural flows, basaltic cones, stratovolcanoes, shallow seismicity and positive gravity anomalies (Figs 1 and 2) (Barberi & Varet 1977; Hayward & Ebinger 1996; Manighetti *et al.* 1997; Cattin *et al.* 2005; Doubre *et al.* 2007a,b). The magmatic segments in the southern Red Sea and western tip of the Aden rift initiated, and probably propagated, after a pulse of volcanic activity at about 2 Ma, but some segments remain undated (Kidane *et al.* 2003; Lahitte *et al.* 2003). These active 'magmatic segments' are similar in size, morphology, structure and spacing to slow-spreading mid-oceanic ridge segments (Hayward & Ebinger 1996). The high heat flux and broad, low form of the Erta'Ale segment led Oppenheimer & Francis (1998) to propose that it is the locus of formation of new igneous crust by dyke intrusions; Doubre *et al.* (2007a,b) and Cattin *et al.* (2005) came to similar conclusions for the Asal rift at the propagating tip of the Gulf of Aden rift.

Geodetic data indicate an average spreading rate of ∼15 mm yr^{-1} across the Nubia–Arabia plate boundary, rates comparable to those in Iceland (Vigny *et al.* 2006). Owing to the sparse station distribution and moderate to small magnitude earthquakes characteristic of this magmatically active zone, earlier seismicity studies in the southern Red Sea region have been restricted to analyses of teleseismic earthquakes (e.g. Sigmundsson 1992; Jacques *et al.* 1999; Hofstetter & Beyth 2003; Ayele *et al.* 2006), a temporary array around the regional capital, Semera (Gresta *et al.* 1997; Hofstetter & Beyth 2003), and a synthesis of historical seismicity (Gouin 1979).

The Dabbahu rift event occurred in the southernmost Red Sea rift north of the Afar triple junction (Figs 1 and 2). The main episode ruptured the length of a previously mapped magmatic segment within the Manda-Hararo rift zone (Barberi & Varet 1977; Hayward & Ebinger 1996; Lahitte *et al.* 2003; see Figs 1 and 2). It began with two m_b 4.5 earthquakes in June and July 2005, followed on September 14 by a m_b 4.7 earthquake (Ayele *et al.* 2007a,b) (Fig. 1). Perhaps coincidentally, the lava lake on Erta 'Ale volcano, 150 km to the northeast of the Dabbahu segment, refilled during

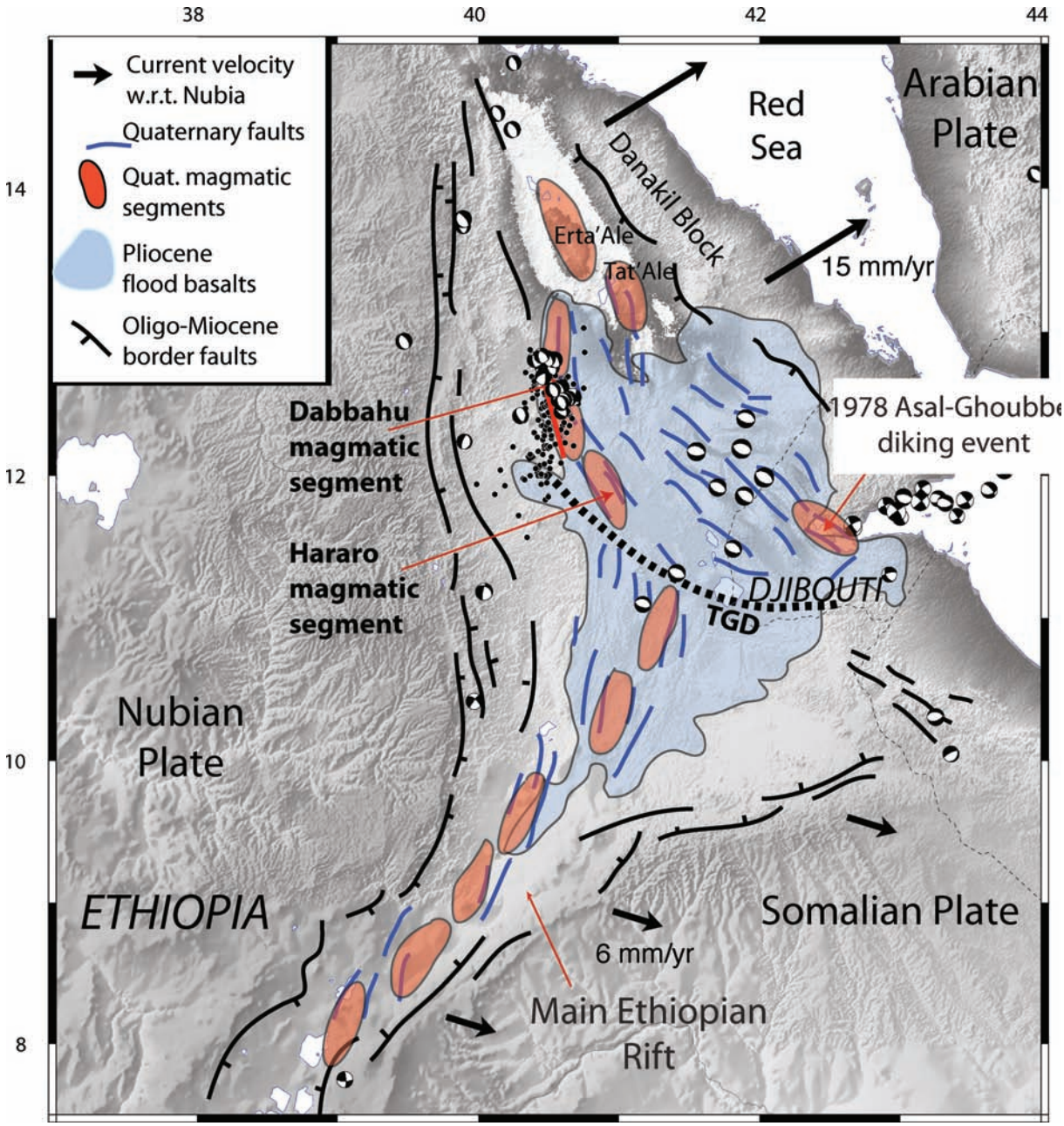

Figure 1. Location of the Dabbahu rift segment within the Afar triple junction zone; major fault zones and Pliocene flood basalts shown schematically. Danakil Block is a microplate between the Nubian and Arabian plates. Red shading indicates ∼50 km-long magmatic segments—zones of dense faulting and aligned Quaternary eruptive centres—the current locus of strain within Afar (after Barberi & Varet 1977; Hayward & Ebinger 1996). Asal-Ghoubbet magmatic segment experienced a seismo-volcanic crisis in 1978 (e.g. Abdallah *et al.* 1979). Arrows show plate motions relative to stable Nubia (Vigny *et al.* 2006; Bendick *et al.* 2006). Focal mechanisms are from the Global CMT database (http://www.globalcmt.org).

this time period (Ayele *et al.* 2007a,b). Nearly continuous seismic activity, including tremor, was registered at station FURI (Addis Ababa) between September 4 and 30, 2005. On September 26, an ∼600-m long, N–S striking vent opened at Da'Ure on the east flank of Dabbahu volcano (Yirgu *et al.* 2006, Figs 1 and 2). The largest of the 163 earthquakes in the NEIC catalogue is the $M_w = 5.5$ event on September 24; the combined seismic moment is an order of magnitude too small to explain the strain estimated from InSAR and structural observations (Wright *et al.* 2006; Rowland *et al.* 2007). The volcanic eruption at Da'Ure and models of InSAR data indicate that the September-October earthquakes were accompanied by the intrusion of a 60-km long dyke with a maximum of 8 m opening (Wright *et al.* 2006; Yirgu *et al.* 2006; Ayele *et al.* 2007a,b). Viscoelastic models of deflation patterns in the InSAR data indicate that no more than 25 per cent of the magma originated from shallow magma chambers beneath the Dabbahu composite volcano and the much smaller Gab'ho rhyolitic centre at the northern tip of the rift segment; deformation was too intense along the dyke intrusion zone to constrain deeper sources (Wright *et al.* 2006; Ayele *et al.* 2007a).

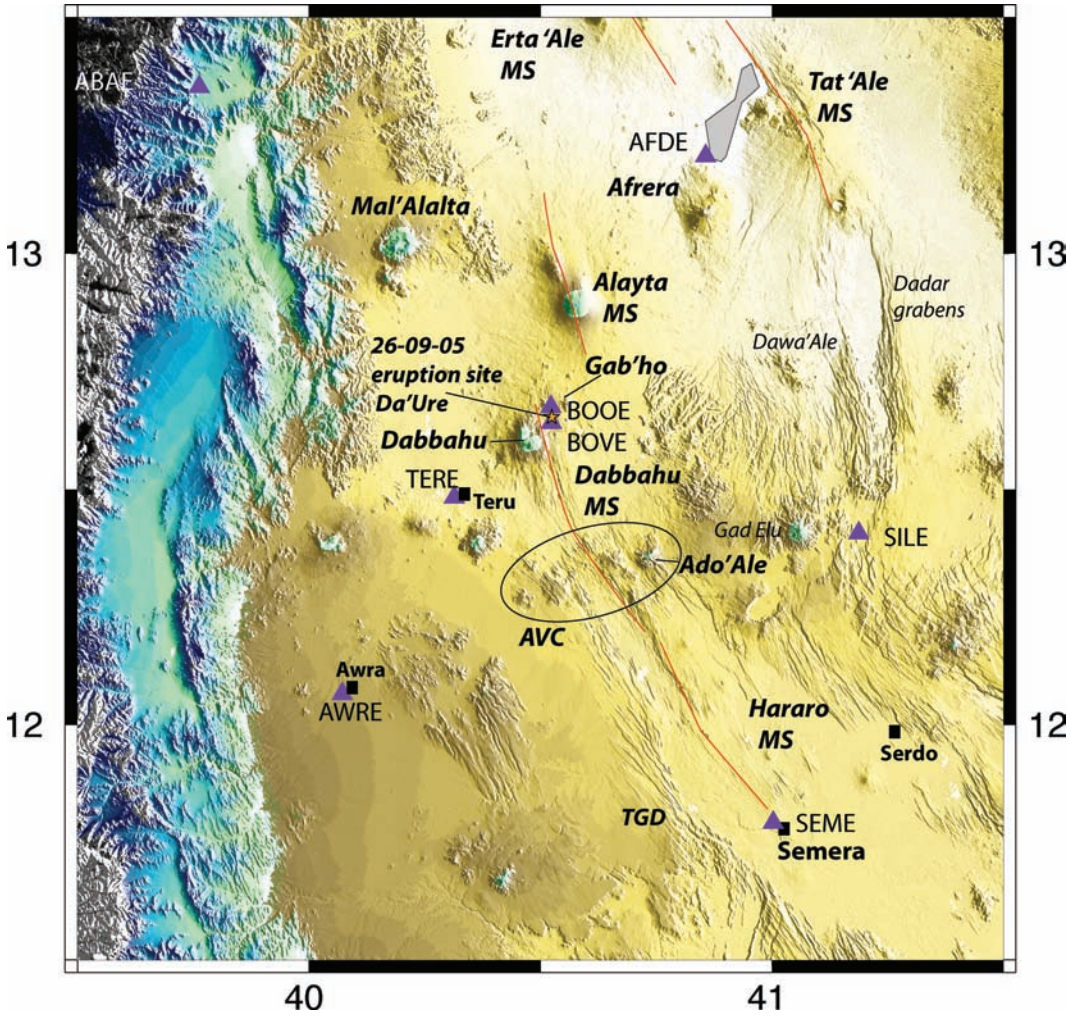

Figure 2. Urgent response seismic array with respect to the Dabbahu and nearby Hararo, Alayta, Tat'Ale and Erta'Ale magmatic segments. Red triangles mark locations of Güralp 6TD seismometers deployed 2005 October 18–19. Star indicates 2005 September 26 eruption site at Da'Ure. MS is Quaternary magmatic segment; D is Dabbahu volcano; TGD is Tendaho-Goba'ad Discontinuity marking the active and ancient boundary between the East African and the Red Sea rifts. Ma'Alalta and Gabho are active volcanoes; Semera is the regional capital of Afar. Aronovitz *et al.* (2007) discuss regional seismicity patterns.

SEISMICITY DATA

Between 2005 October 19 and 21, we deployed six Güralp 6TD broad-band seismometers in or near villages to the east and west of the Dabbahu–Hararo rift segments and one in the regional capital, Semera (Fig. 2). Three seismometers were installed near the Da'Ure eruption site to monitor what we originally thought was a flank eruption of Dabbahu volcano. An unguarded site at ∼12°18′N was vandalized, limiting the resolution of the array in the southern part of the segment.

Instruments recorded at a sampling rate of 50 Hz. High frequency (>1 Hz) cultural noise was very low at BOOE, BOSE and BOVE near the vent site; the other sites in villages were noisy during early evening when generators were used (Fig. 3). BOOE, BOVE and BOSE show up to 20 shallow volcano-tectonic earthquakes and tornillos per hr until 2006 January, when activity became more episodic. The harsh field conditions and rapid deployment led to instrument failures and a decrease in operational seismic stations over time. Additional data over parts of this time period were acquired from the permanent station DESE maintained by the Geophysical Observatory of Addis Ababa University. The temporary array allows accurate location of low magnitude seismicity not possible from permanent regional stations (ATD, FURI).

Arrival time analysis

Arrival times of *P* and *S* phases were measured manually on traces filtered using a Butterworth bandpass filter (1–15 Hz). Arrival times of *P* phases were assigned a quality factor of 0, 1, 2 or 3 according to estimated measurement errors of 0.05, 0.1, 0.15 and 0.2 s, respectively. *S*-wave quality factors of 0, 1, 2 and 3 were assigned to arrivals with estimated measurement errors of 0.1, 0.175, 0.25 and 0.3 s, respectively.

Earthquake locations

A total of 1939 earthquakes were recorded on four or more instruments during the period 2005 October 19 to 2006 April 1; 961 earthquakes occurred during the first month of the deployment. Earthquakes first were located using Hypo2000 (Klein 2002). We adopt the 3-layer velocity model of Jacques *et al.* (1999), derived from earlier refraction studies in Afar (Berckhemer *et al.* 1975;

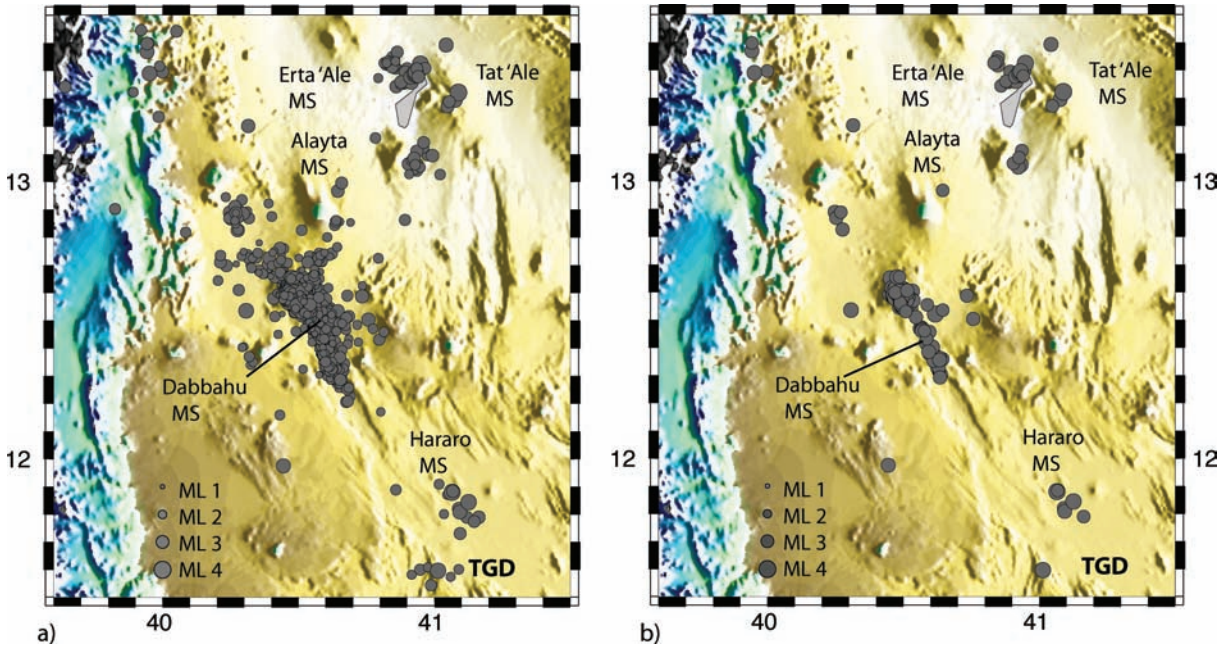

Figure 3. (a) All earthquakes from the period 2005 October 19 to 2006 April 1, located using HYPO2000 (Klein 2002) with symbol scaled to magnitude. (b) Earthquakes of $M_L \geq 3$ occur along the length of the Dabbahu segment. MS is magmatic segment.

Ruegg 1975). Fig. 3 shows the locations of the full data set, prior to relocation using the double-difference method of Waldhauser & Ellsworth (2000). The vast majority of events occurred adjacent to, or along the length of the Dabbahu rift segment (Figs 2 and 3). Swarms were also observed between the Dabbahu and Alayta magmatic segments, between the Dabbahu segment and the western Red Sea escarpment, along the Tendaho-Goba'ad Discontinuity separating the Main Ethiopian (East African) and Red Sea rifts and along the Tat 'Ale magmatic segment (Fig. 3). This paper focuses on the seismicity within the Dabbahu segment; later papers will examine the Dabbahu rift within the regional plate kinematic setting.

Relocation procedure

Subsets of the output from Hypo2000 were relocated relative to one another using the double difference earthquake location algorithm of Waldhauser & Ellsworth (2000). In this method, traveltimes of pairs of earthquakes recorded at the same stations are compared with calculated traveltimes. The residuals between calculated and observed times are minimized by adjustments of vector differences between hypocentres (e.g. Préjean *et al.* 2003). The comparison of common traveltime paths eliminates the need for station corrections and *a priori* knowledge of local velocity variations. The residuals between double difference pairs at each station were minimized by weighted least squares using a singular value decomposition algorithm (Waldhauser & Ellsworth 2000).

Given the large number of closely spaced events but sparse and wide station spacing, we chose the strict criteria of eight or more phase pairs for all solutions. We subdivided the data by region to improve locations within discrete clusters. In total, 736 events with a minimum of eight or more phase pairs were relocated (Fig. 4). The shallowest earthquakes beneath Dabbahu volcano, which rises more than 700 m above stations BOVE and BOSE, appear as air quakes, explaining some of the differences between Figs 3 and 4. Position errors range from 50 m near Dabbahu to 3000 m for events at the southern end of the Dabbahu magmatic segment. Depth errors are less than <500 m near the northern end of the array, but increase to 3000 m at the array limits.

Magnitude determination

Local magnitude was estimated using the maximum body wave displacement amplitudes measured on a simulated Wood–Anderson seismograph and distance corrections terms of Keir *et al.* (2006b) (Fig. 3). The data set is complete for events larger than $\sim M_L = 2.5$, but the time-series presented in this first report is too short to draw any further insights. Over the time period October 19 to April 1, 201 earthquakes with $M_L > 3$ occurred in the Dabbahu, Tat 'Ale, and Manda Hararo segments, as well as the western rift margin (Fig. 3b).

Focal mechanisms

We computed earthquake focal mechanisms for comparison with field and remote sensing analyses of fault and intrusion patterns. The best fit double couple component to the source mechanisms were computed from *P*- and *SH*-wave polarities using the grid search algorithm FOCMEC (Snoke 2003). The clvd component of the source mechanisms cannot be constrained due to insufficient near source seismic stations. All fault plane solutions have a minimum of seven *P*-wave polarities located in at least 3 quadrants of the focal sphere. Polarity errors of both *P*- and *SH*-waves were not tolerated in the grid search algorithm. We determined 13 well constrained and unambiguous fault plane solutions that have a maximum 20° uncertainty in strike and dip of both nodal planes (Table 1, Fig. 5). Earthquakes for which solutions could be determined occurred between October and December 2005 and have local magnitudes (M_L) that range from 3.0 to 4.0. Solutions for earthquakes in 2006 could not be constrained due to failure of several seismic stations, coupled with the reduction in earthquake magnitude with time after the September 2005 intrusion. The spatial variation in

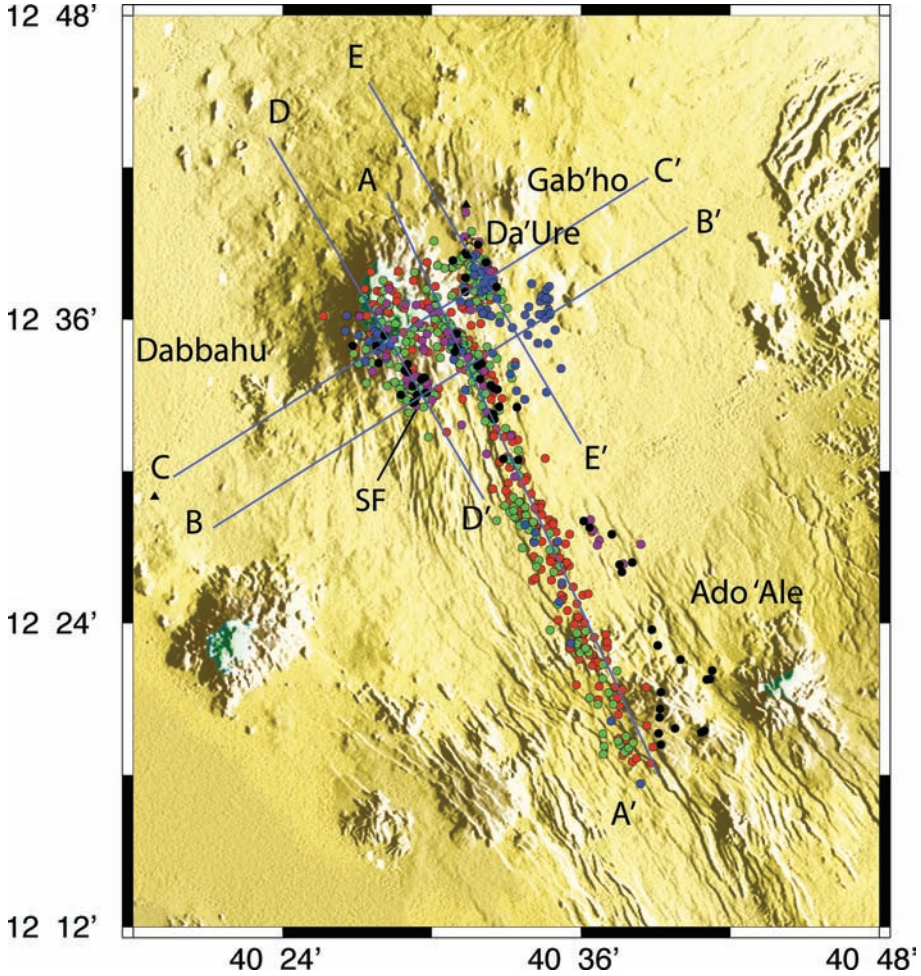

Figure 4. Earthquake epicentres relocated using the double difference method of Waldhauser & Ellsworth (2000). A-A′, B-B′, C-C′, D-D′ E-E′ mark the locations of topography and seismicity profiles shown in Figs 7 and 8. Colours signify temporal variations: red, 2005 October 19–31; green, 2005 November 1–30; blue, 2005 December 1–31; violet, 2006 1–31; black, 2006 February 1–March 30. Ado 'Ale, Dabbahu, Gab'ho are silicic volcanoes.

Table 1. Focal mechanisms for selected events.

ID	Date	Time	Lon	Lat	Depth	M_l	Strike	Dip	Rake
1	05/10/20	16:38	40.581	12.472	4.7	3.65	337	51	−75
2	05/10/20	19:49	40.631	12.316	3.1	3.27	168	38	−70
3	05/10/20	23:00	40.513	12.604	1.9	2.91	0	48	−82
4	05/10/22	22:56	40.609	12.376	3.6	3.45	328	46	−82
5	05/10/23	00:43	40.499	12.597	1.5	3.13	7	44	−81
6	05/10/23	04:54	40.502	12.595	2.1	3.76	200	80	−12
7	05/10/24	23:48	40.463	12.613	2.0	3.83	332	48	−87
8	05/10/27	14:39	40.459	12.632	1.9	3.46	344	50	−83
9	05/10/27	16:21	40.614	12.368	1.6	3.49	146	40	−82
10	05/11/01	11:22	40.607	12.403	5.1[a]	3.47	341	52	−71
11	05/11/09	21:37	40.512	12.581	1.7	2.94	356	46	−82
12	05/11/11	05:22	40.461	12.615	4.9[a]	3.86	158	46	−82
13	05/12/17	20:48	40.500	12.548	3.2[a]	3.25	91	87	9

[a]Location depth from Hypoinverse 2000.

fault slip patterns are discussed with regard to discrete earthquake clusters in the subsequent section.

Seismogenic layer thickness

The depth histogram for the relocated events is bi-modal, with peaks at 2–3 km and 4–6 km subsurface (Fig. 6). Our velocity-depth relation has a step at 3 km subsurface; the bimodality is in part an artefact of the simple velocity model used in this region of magma intrusion (Jacques *et al.* 1999). About 75 per cent of the shallowest events occurred beneath Dabbahu volcano.

DABBAHU SEGMENT SEISMICITY PATTERNS

The discussion below focuses on the well-determined events relocated using the double difference method (Fig. 4). Impulsive and hybrid earthquakes cluster along the ∼60-km long, ∼8-km wide zone of deformation delineated in InSAR data from the major 2005 September activity (Wright *et al.* 2006; Ayele *et al.* 2007a b) and noted from eye witness accounts and visual inspection by helicopter (Yirgu *et al.* 2006; Rowland *et al.* 2007; see Figs 4, 5 and 7–9). The dyke intrusion zone is characterized by 3-km wide band of earthquakes with hypocentres contiguous between ∼8 km and the surface (Fig. 7). Depths are variable along the length of the dyke. This band of seismicity narrows east of Dabbahu and curves NW towards the volcanic peak, where it merges with a shallow zone of seismicity beneath the central peak (Figs 4, 5 and 7–9).

A second persistent swarm marks the Dabbahu volcanic peak. Two more tightly clustered, persistent swarms lie on the southern flank of Dabbahu and the region south of the Da'Ure vent (Figs 3 and 7–9).

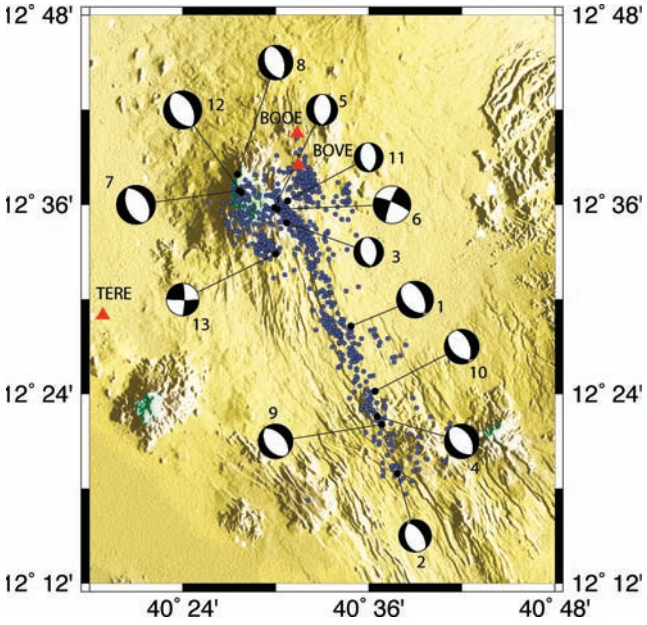

Figure 5. Focal mechanisms for selected events within the Dabbahu rift segment with seven or more *P*-wave arrivals recorded during the period 2005 October 19 to 2006 March 30. Numbers referred to events in Table 1. Symbol size is scaled to magnitude. Triangles denote seismometer locations.

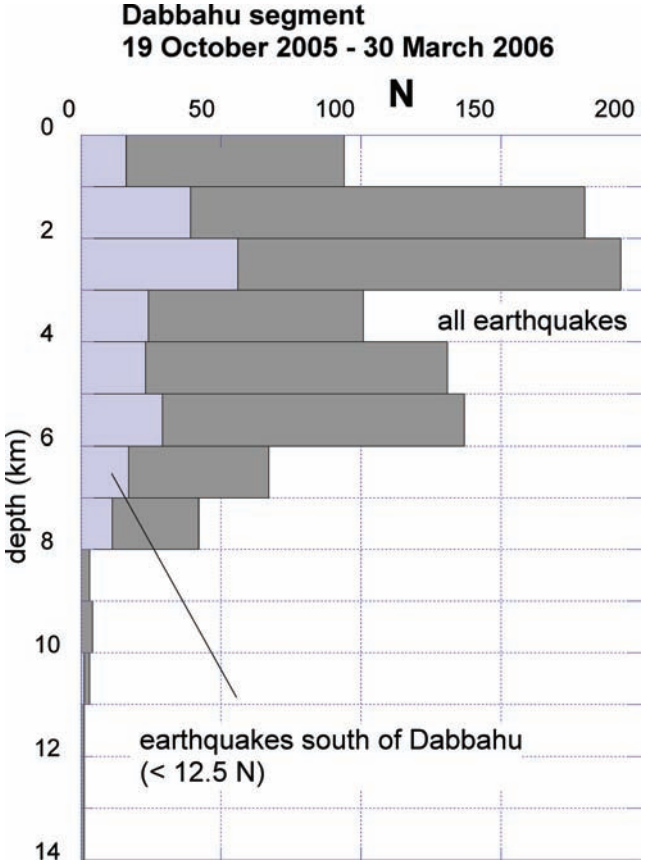

Figure 6. Histogram of focal depths for the double difference solutions of the best-located subsets of the 2005 October 19 to 2006 April 1 data set (Fig. 4). Light grey patterns denote depth range of events south of Dabbahu volcano (12°30′N), dark grey represents the full data set for the Dabbahu segment. Note that the velocity depth model has a step increase at 3 km subsurface.

The dyke zone, south flank subsidence zone, Da'Ure vent and Dabbahu peak show persistent seismicity from October to December (Fig. 4). Notable, however, is the seismicity on the eastern flank of the Dabbahu segment during the period 2006 January to April. This shallow seismicity (≤5 km) occurs along NW-trending faults and across the rifted Ado 'Ale volcano complex at ∼12°22′N (Fig. 4).

Comparisons with InSAR and continuous GPS data from Dabbahu and Gab'ho over approximately the same time period (2005 October 28 to 2006 April 21) reveal strong correlations between the spatial patterns of seismicity and the surface deformation (Figs 9 and 10). Persistent seismic swarms at two sites on Dabbahu volcano coincide with areas of faulting, subsidence, and/or uplift in the interferograms. Below and in Fig. 11 we discuss each of the discrete clusters in light of focal mechanisms, seismogenic layer thickness, InSAR and GPS data and field observations.

Dyke zone

The intensely clustered events reproduce the length of the rupture evident as closely-spaced interference fringes in the interferogram of 2005 October 28 to 2006 April 21 (Fig. 9). The zone of rupture spatially coincides with the 2005 September dyke intrusion zone (Wright *et al.* 2006) but with an order of magnitude smaller displacement. Earthquake epicentres, like the recently active faults, form a right-stepping en echelon array of NW-striking segments (Rowland *et al.* 2007), giving the dyke an apparent NNW-trending orientation. Closely-spaced, NNW-trending interference fringes and displacements from subpixel resolution SPOT images show the same apparent right-stepping en echelon pattern as the relocated earthquake swarms (Grandin *et al.* 2007; Barisin *et al.* 2007) (Fig. 9). These patterns indicate continued dyke intrusion and rift opening, with activity decreasing markedly by 2006 January (e.g. Fig. 4).

The tightest cluster lies at the northern end of the earlier dyke where the trend changes to NW on the eastern flank of Dabbahu volcano. There is a clear gap in seismicity between the dyke zone and the September 26 vent site (star, Figs 4, 8 and 9). Further insights on the interaction between the dyke intrusion zone and the crustal magma reservoirs at the northern end of the segment are outlined below and integrated into the discussion.

Rowland *et al.* (2007) use field calibrated high resolution images to document slip on both NW and N–S oblique-slip faults linking en echelon fault arrays. Pre-existing faults above this zone show up to 3 m of additional displacement, but it was impossible to determine whether the slip was accrued in single or multiple earthquakes for most faults. Newly formed monoclines, open fissures and collapse structures are common above this seismogenic zone (Rowland *et al.* 2007).

Focal mechanism solutions show slip along steep normal faults striking N40°W, parallel to active faults. The focal plane orientations shift to a more northerly alignment (N20°W to N10°E), where the dyke curves westward beneath the Dabbahu volcanic edifice (Fig. 5).

The depth extent of seismicity decreases from north to south along the length of the dyke, shallowing to ∼6 km above the zone of magma intrusion at ∼10 km subsurface inferred from geodetic models (Figs 4 and 7). The two interference fringe lobes centred on the dyke at ∼12°18′N indicate ∼20 cm of inflation over this time period (Fig. 9). This deeper source region is largely aseismic. The seismogenic layer thickness thins to the south toward Ado'Ale volcano and the two broad lobes of uplift. This area was the locus

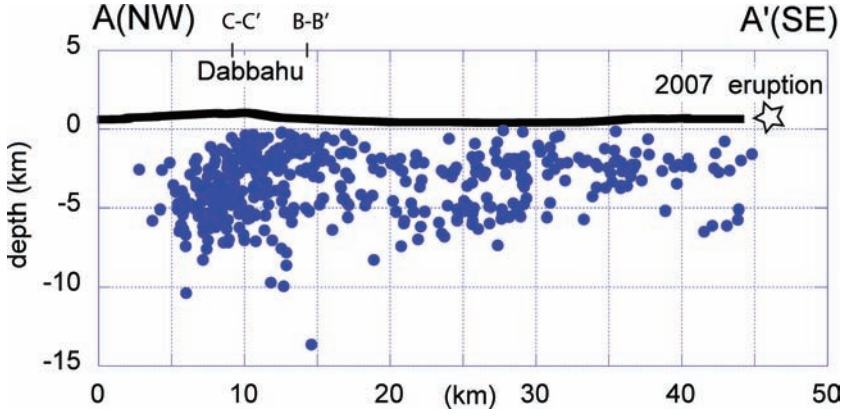

Figure 7. Seismicity within a ≤4 km swath projected onto the line of Profile A-A′ shown in Fig. 4. Crossing points of Profiles B and C are indicated above the graph. The shallowest events correspond to surface breaks described in Rowland *et al.* (2007). Patterns in the Dabbahu complex are shown in more detail along- and across-axis profiles in Fig. 8.

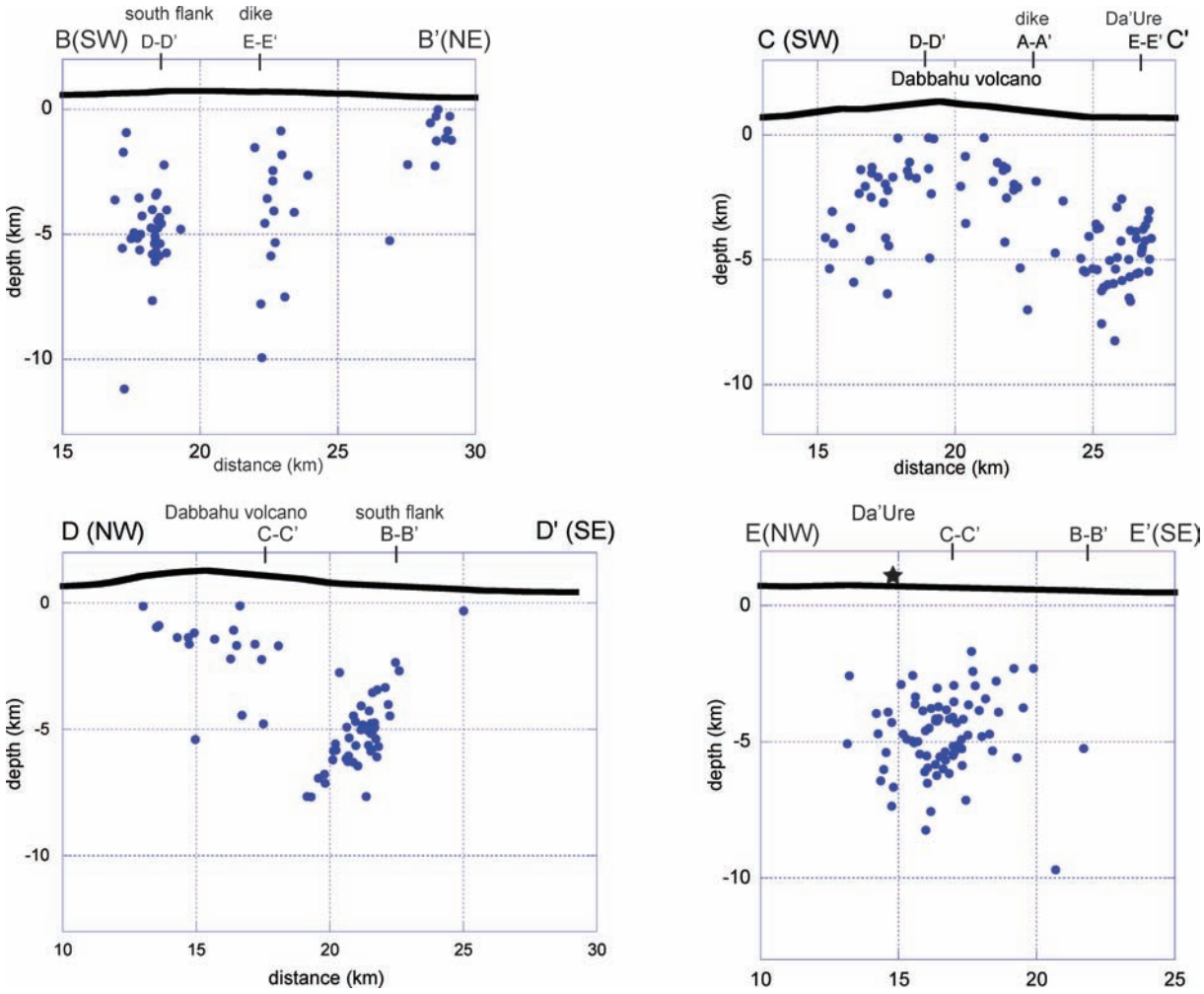

Figure 8. Seismicity in ≤2 km-swaths projected on the line of profiles B-B′, C-C′, D-D′, and E-E′ shown in Fig. 4. All profiles are shown at true scale to enable correlations with focal mechanisms and fault slip data. Crossing points of profiles are indicated above the profile (Figs 4 and 7).

of later dyke intrusion events in 2006 June, July and September interpreted from seismicity and InSAR patterns (Keir *et al.* submitted), suggesting that magma recharge and continued dyke intrusion occurred near the southern end of the segment where the array was only able to detect larger magnitude events.

Dabbahu peak

Teleseismic events from the September activity, albeit with epicentral errors of ∼10 km (Ayele 2007b), clustered around Dabbahu and Gabh'ho volcanoes prior to the eruption on September 26 when

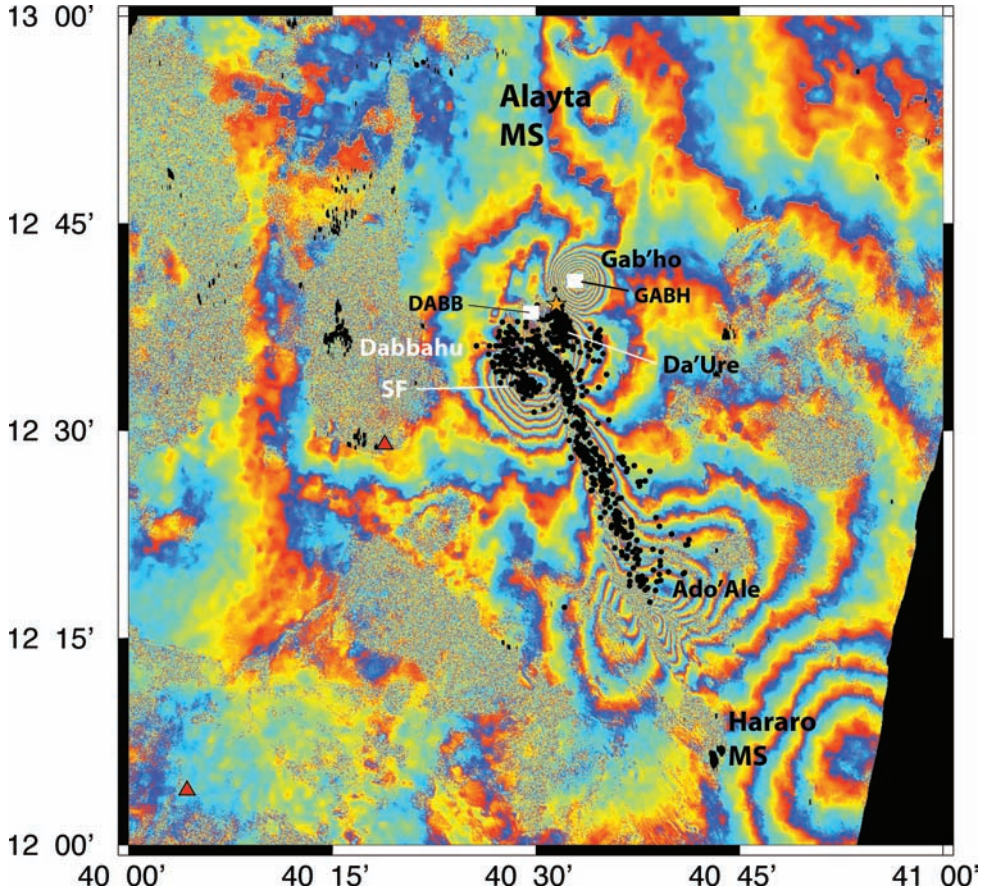

Figure 9. Earthquakes from the period 2005 October 19 to 2006 April 1, relocated using the double difference method displayed on radar interferogram (Envisat standard track 49, beam mode IS2) spanning the interval 2005 October 28 to 2006 April 21. Each colour cycle, blue–yellow–red is equivalent to a range increase of 2.8 cm. Orange star is the 2006 September 26 eruption site; red triangles are seismic stations. SF is south flank of Dabbahu cluster; Ado'Ale, Dabbahu and Gab'ho are silicic volcanoes. DABB is Dabbahu GPS site; GABH is Gab'ho GPS site. In this descending interferogram, range increases can result from subsidence and/or westward motion. Range decreases occur on the northern slopes of Dabbahu volcano, and around Gab'ho volcano, indicating uplift. Note the two broader lobes of deformation on either side of the rift at the 12° 15′N (near Ado'Ale volcano) and the NW striking, en echelon pattern of seismicity clusters and interference fringes along the dyke south of Dabbahu volcano, indicating continued dyke intrusion (Fig. 4).

activity spanned the ∼60 km length of the Dabbahhu magmatic segment (Wright *et al.* 2006; Ayele *et al.* 2007a,b).

A diffuse cluster of seismicity underlies the peak elevations (>1000 m) of Dabbahu volcano. Earthquakes form a broad lens of radius ∼10 km at ∼2.5 km subsurface; a few earthquakes occurred at deeper levels (Figs 4 and 8). Radar interferometry indicate a broad zone of slow uplift across the northern side of the Dabbahu complex, but the continuous GPS data from Dabbahu's northern flank show reinflation beginning in April (Fig. 10a). The intense, persistent swarms of seismicity in the Dabbahu edifice suggest that pressure remained high in the shallow crustal reservoir even after the flank eruption at Da'Ure (e.g. Feigl *et al.* 2000). Wright *et al.* (2006) simulated the September-October InSAR deformation patterns with a deflating magma body at 5 km depth; our hypocentral locations suggest the sill-like melt zone lies between 3 and 5 km.

Focal mechanisms in the period October to December correspond to slip along NW to N–S-trending normal faults, subparallel to focal mechanisms along the length of the dyke. A shallow (<1 km depth) strike-slip event occurred in the zone of interaction between the dyke and the Dabbahu magma chamber(s) on November 11 (Fig. 5, Table 1). The *p*-axis of this single event is rift-parallel, possibly indicating that the stress field induced by the dyke was greater than the tectonic stress in this zone of interaction between the dyke and the Dabbahu magma chamber(s) (e.g. Roman & Heron 2007).

Dabbahu South Flank

A dense cluster of earthquakes marks the core of a broad zone of subsidence in the interferogram (Fig. 9); ∼25 cm of subsidence occurred between 2005 October and 2006 April. This ∼4-km long, E–W elongate cluster defines a plane dipping ∼45° to the NE between 2 and 8 km subsurface (D-D′, Fig. 9). The only focal mechanism within this cluster is a strike-slip mechanism with E–W and N–S focal planes, consistent with a local stress change induced by dyke intrusion (e.g. Bonafede & Danesi 1997, see Fig. 5, Table 1). The northward dipping cluster of seismicity between 2 and 8 km subsurface may mark a magmatic connection between a deflating mid-crustal deflating magma chamber that feeds the inflating sill-like chamber within the Dabbahu edifice.

Da'Ure vent site

An elliptical-shaped cluster lies beneath the Da'Ure vent site to the east of Dabbahu volcano (Fig. 3). The small rhyolitic domes and cones of the Da'Ure region are also a zone of subsidence;

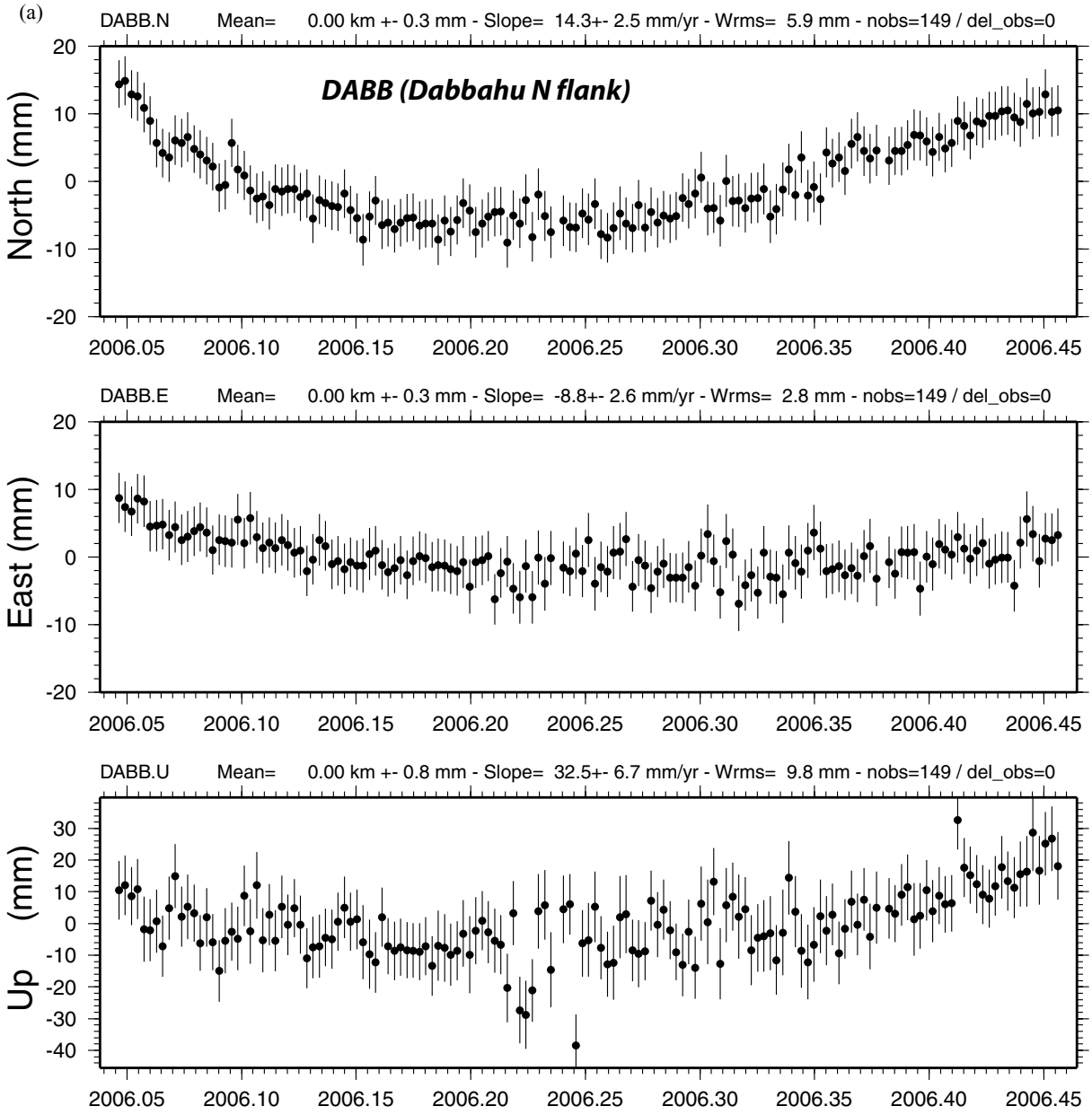

Figure 10. Daily averages of E, W and up components of plate motion from continuous GPS sites on Dabbahu and Gab'ho volcanoes (Figs 2 and 9). Errors are 2σ, horizontal axis is Julian day/365. (a) Site DABB on Dabbahu's northeastern flank shows slow, southward-directed subsidence between January and April, consistent with the InSAR observations of subsidence on Dabbahu's south flank (Fig. 9). Inflation begins in April, with slow uplift by 2006 June. (b) Site GABH on Gab'ho volcano showing steady inflation from 2006 January to June.

the more broadly-spaced fringes suggest a deeper and/or broader source than beneath the 'South Flank' zone (Fig. 9). There are no focal mechanisms for the relatively small magnitude Da'Ure events. Cross-sections E-E′ and C-C′ cross this cluster; the NW–SE profile shows a 2-km wide shadow zone ringed by tightly-clustered events at 5 km subsurface (Fig. 8). This feature is robust with varying azimuth; it appears to be elongate in a NW–SE direction. Petrological analyses of the erupted rhyolites and ash suggest heating of a source body at depth <6 km with an influx of basaltic magma (Yirgu *et al.* 2006); models of InSAR data also suggest a deflating source body at ∼5 km subsurface fed the surface eruption and contributed to the dyke (Wright *et al.* 2006). Considering the independent constraints on magma storage beneath the Da'Ure region, we propose that the halo of seismicity may mark hydraulic fracture in the hot weak zone of rock surrounding a <1-km wide, aseismic magma chamber.

Gab'ho volcano

Gab'ho is a small rhyolitic eruptive centre northeast of the Da'Ure vent site (Figs 2 and 4). The comparatively crude (*ca.* 30 km) relocations of teleseismic earthquakes preceding the eruption at Da'Ure on September 26 cluster between Dabbahu and Gab'ho (Wright *et al.* 2006; Ayele *et al.* 2007a, b). Local Afari pastoralists witnessed *ca.* 0.5 m slip along a NNW-striking normal fault on September 26 (Yirgu *et al.* 2006), and interferograms showed deflation (Wright

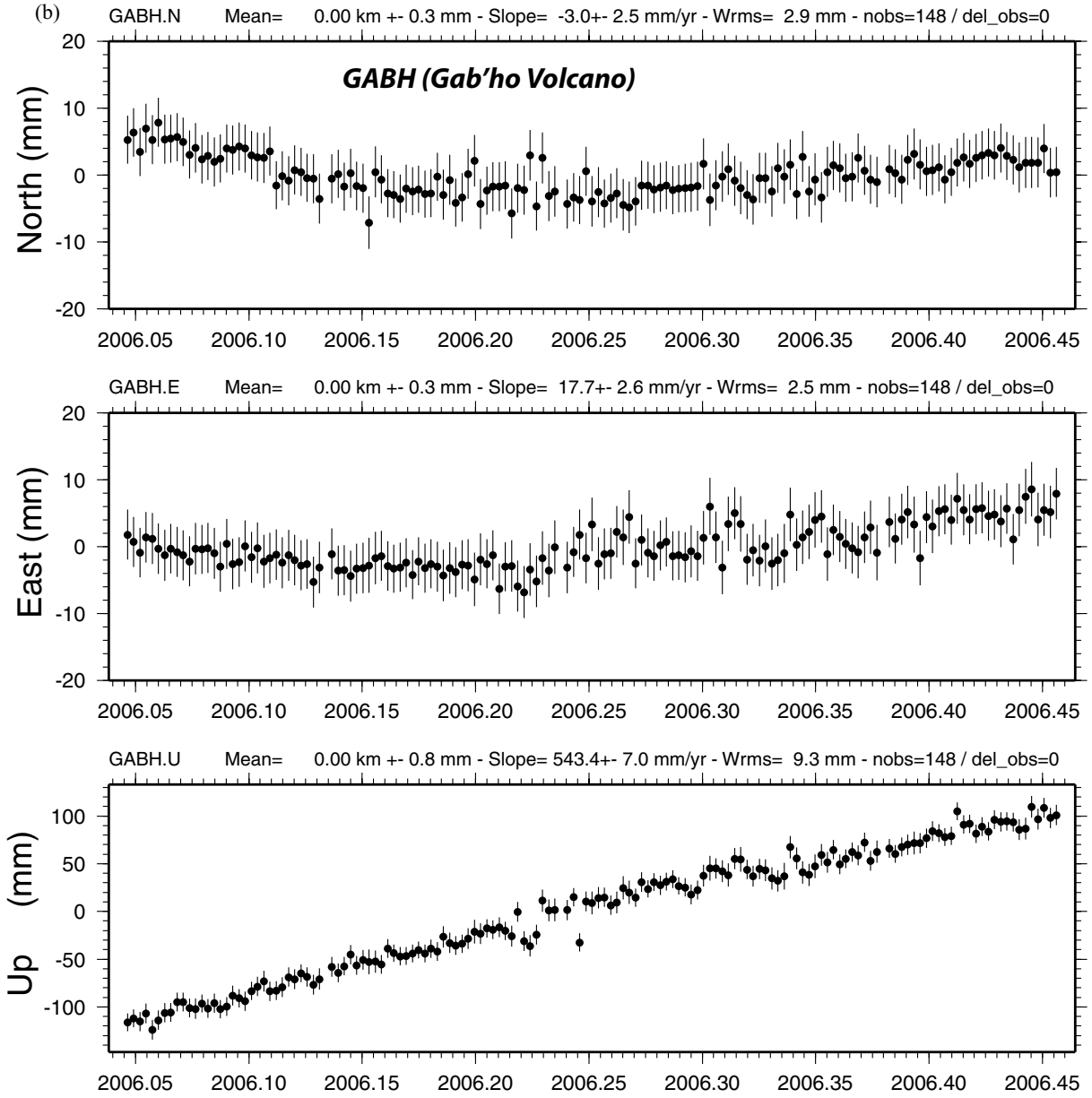

Figure 10. (*Continued.*)

et al. 2006). During our array deployment, this area was largely aseismic as the volcano re-inflated; interferograms from November to April show ∼280 mm of inflation at Gab'ho (Fig. 9). The GPS time-series from January to April also shows steady uplift of Gab'ho at a rate of ∼543 mm yr^{-1} (Fig. 10b). The temporal changes in uplift (subsidence followed by steady inflation) and aseismic character during the inflation period suggest that the September earthquakes and magma withdrawal reduced the stress in the crustal lid above the Gab'ho magma chamber during the September-October 2005 seismo-volcanic crisis, enabling aseismic magma inflation beneath Gab'ho volcano.

Eastern flank seismicity

The well-located, shallow (<3 km) events from January to March lying on the eastern flank of the Dabbahu rift segment closely parallel the 2005 September dyke intrusion zone. These swarms are absent on the western flank. The pattern of these eastern flank earthquakes parallels the contours of interference fringes in Fig. 9; they occurred after activity dropped below the detection level in the central and southern parts of the dyke (Figs 4, 8 and 9). The eastern flank events may mark a period of stress adjustment after the cessation of dyke intrusion, an interpretation to be tested with models of geodetic data.

DISCUSSION: MAGMA INTRUSION PROCESSES

Additional insight comes from comparison to tectono-magmatic events in Iceland and the Asal rift at the western tip of the Aden spreading ridge. The 1975–1989 Krafla rifting episode occurred along a pre-existing, 70-km-long segment of the Northern Rift Zone

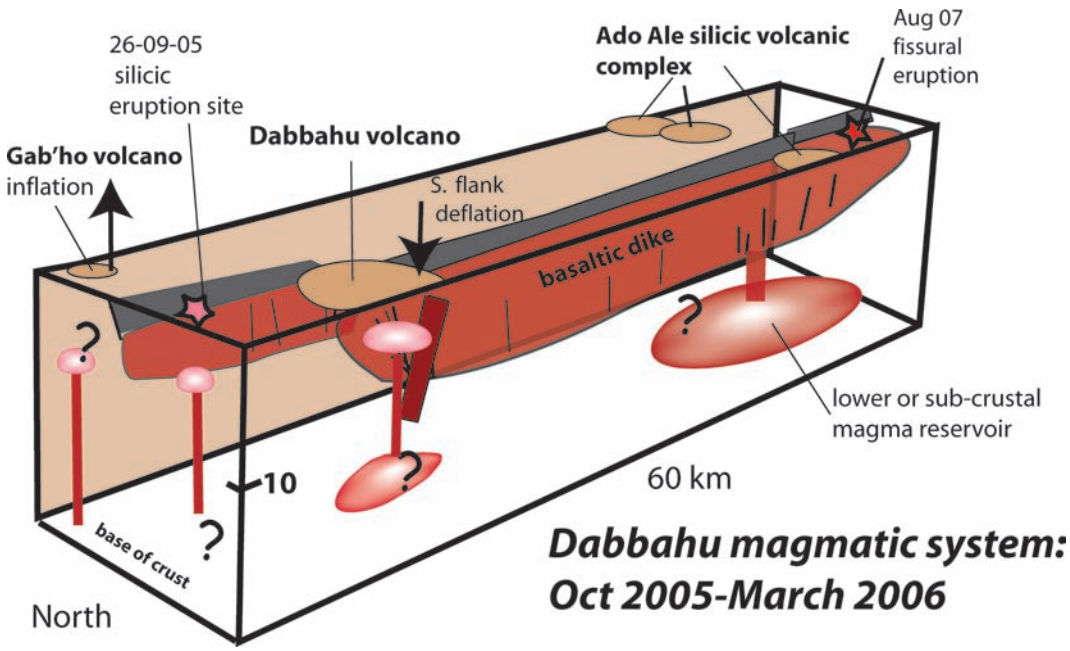

Figure 11. Working model of magma migration through the crust beneath the Dabbahu rift segment, based on seismicity, InSAR, GPS and structural observations from along the length of the Dabbahu segment. Topographic relief has been removed for simplification; volcanoes are indicated by beige ellipses. Arrows indicate vertical crustal movements over the period October 19–April 21 from GPS and InSAR. The red blade-like dykes correspond to the seismogenic zones: the main dyke zone that curves into the Dabbahu edifice, and a second dyke to the east. Pink ellipses are magma chambers beneath Gab'ho, Da'Ure and Dabbahu. The location of lower crustal/upper-mantle source zones feeding the dykes and magma chambers is loosely constrained by the InSAR data and subsequent deformation in 2006 (Keir *et al.* submitted). The deflation of Dabbahu and Gab'ho during/after the dyking episode indicates some connectivity between the basaltic dykes and the silicic magma chamber beneath Dabbahu (Wright *et al.* 2006). The deep red semi-circular, northward-dipping zone of persistent seismicity may mark a collapsing pipe or fault above a mid-crustal magma reservoir.

in Iceland (e.g. Bjornsson *et al.* 1977; Einarsson 1991; Tryggvason 1994). Fault slip was $\leq$2 m in the first, largely intrusive event, which was characterized by earthquakes as deep as 10 km, and migrating swarms at its leading edge (Einarsson & Brandsdottir 1980). Successive dyking events propagated shorter distances along the rift and were more effusive. Much of the magma feeding the dykes came from a $\sim$8 km-wide magma reservoir between $\sim$2.7 and 5 km subsurface beneath Krafla caldera near the centre of the rift segment (e.g. Brandsdottir *et al.* 1997). The dimensions of the Krafla chamber are similar to those inferred beneath Dabbahu (Fig. 11). Geodetic data were unavailable until 8 yr after the start of the sequence, but surface deflation of $\sim$5 cm yr^{-1} was measured at the power plant within Krafla caldera (e.g. Tryggvason 1994; Foulger *et al.* 1992). Observations since the end of the rifting cycle provide insights into the interseismic magma cycle. A deep zone of magma ponding at the crust–mantle boundary (21 km) has been inferred from models of radar interferometry for the period 1993–1999 (de Zeeuw-van Dalfsen *et al.* 2004) and theoretical considerations (Gudmundsson 1995, 2006).

As in the Krafla episode, the 1978 Asal–Ghoubbet event commenced with a $m_b = 5.3$ earthquake near the centre of a 60-km long segment followed by a week-long volcanic eruption at Fieale volcano in the onshore sector of the rift and swarms of shallow earthquakes along a $\sim$20-km-long part of the rift segment (e.g. Abdallah *et al.* 1979; Doubre *et al.* 2007a,b). Cattin *et al.* (2005) and Doubre *et al.* (2007b) interpret the spatial and temporal pattern of deformation derived from classical GPS and seismicity during the first 5 yr after the 1978 event as continued dyking, rather than viscoelastic relaxation of the extended plate. As in the 2005 September Dabbahu dyke intrusion, the seismic energy release cannot account for the plate opening; syn- and post-crisis deformation occurs largely aseismically (Doubre *et al.* 2007b). Seismicity since 1978 clusters at 3–5 km depth beneath Fieale volcano, the top of the inferred magma chamber (Doubre *et al.* 2007a).

The dyke intrusion events at Krafla (Einarsson & Brandsdottir 1980; Brandsdottir *et al.* 1997), and Asal (Abdallah *et al.* 1979; Doubre *et al.* 2007b) were sourced from a shallow crustal magma reservoir near the centre of the rift segments. The volume of magma intruded in the September 2005 initial Dabbahu crisis is twice that of the 9-yr Krafla cycle, arguing against a subtle, as yet unnoticed shallow reservoir near the middle of the Dabbahu segment; neither the InSAR data nor the seismicity indicate subsidence or collapse as seen at Dabbahu volcano (e.g. Fig. 9). Simple elastic models of Wright *et al.* (2006) and Ayele *et al.* (2007a,b) indicate that $\sim$20 per cent of the magma was sourced from Dabbahu and Gab'ho magma chambers. Was the remaining magma volume injected from deeper source(s) along the length of the Dabbahu segment? The InSAR data, as well as the along-axis seismicity patterns, suggest a deep source beneath 12°18′N feeding and maintaining the Dabbahu rift segment (e.g. Figs 7, 9 and 11). A fissural eruption in August, 2007 occurred near the southern tip of the segment (Yirgu 2007), and seismicity and InSAR patterns show continued dyking centred around this same zone during 2006 and 2007 (Keir *et al.* submitted). Shallow reservoirs near the centre of the segment have existed during past rifting cycles; the silicic volcano complex at Ado 'Ale has been rifted apart by previous crises in the Dabbahu segment, as have the even older silicic centres forming a chain 10 km off-axis (Rowland *et al.* 2007) (Fig. 2). The repeated episodes of silicic volcanism near the mid-segment suggest that the along-axis segmentation is produced by enhanced upwelling, as along

mid-ocean ridges (e.g. Whitehead *et al.* 1984; Macdonald 1998) (Figs 2 and 11). Longer-term regional geodetic and seismic monitoring programmes are designed to address this question.

Why does the Dabbahu segment have an active silicic volcano complex at its northern tip, unlike the Asal-Ghoubbet and Krafla rift zones? One explanation relates to the along-axis arrangement of discrete magmatic segments in this incipient rupture zone (Figs 1 and 2). The axis of the rift shows little deviation between the Dabbahu segment and the Hararo segment to the south, but the Alayta segment to the north is offset to the east of the Dabbahu segment (Figs 1 and 2). This along-axis geometry places the northern tip of the Dabbahu segment against colder, thicker lithosphere, inhibiting the lateral propagation of dykes, leaving magma to pond in crustal reservoirs (e.g. Figs 1 and 2). Along the length of the less evolved Main Ethiopian rift, silicic complexes occur at the tips of magmatic segments with a right-stepping, en echelon geometry (e.g. Wolfenden *et al.* 2005; Casey *et al.* 2006). Alternatively, the Dabbahu volcano complex may have existed prior to the localization of strain and magmatism along the Dabbahu rift segment at 1–2 Ma; it may have been 'captured' by the current rift zone configuration.

Considered together, the distribution, magnitude and mechanism of seismicity, and the InSAR and GPS deformation all suggest that magma injection continued along the length of the ∼60 km-long Dabbahu rift segment until the end of 2005 December. The September events, most of which occurred between September 24 and 26, did not end in fissural eruptions, suggesting that tectonic stress levels remained high enough to drive further intrusions.

CONCLUSIONS

Dense swarms of seismicity along the 60-km length of the Dabbahu rift segment characterize the first 7 months of activity recorded on a temporary network after the start of the 2005 Dabbahu seismo-volcanic crisis. Along the length of the segment, focal depths determined using the double difference method lie between 10 km and the surface. Considering the large volume (∼2.5 km^3) of magma intruded during the 2005 September crisis, we interpret the zone of seismicity as failure on the sides and above the dyke injection zone. Focal mechanisms show rift-normal opening. The persistent seismicity, InSAR, continuous GPS and structural patterns all suggest that magma injection continued at least 3 months after the main episode. Unlike earlier dyke intrusions in Krafla and Asal-Ghoubbet (Afar), there is no shallow magma reservoir feeding the dykes; InSAR patterns and the shallowing of seismogenic layer suggest the dyke was fed from the base of or beneath the crust, near the centre of the segment at 12°18′N. The deep roots of the dyke within the aseismic lower crust may have remained open from 2005 September to December.

Persistent seismic swarms at two sites on Dabbahu volcano coincide with areas of deformation identified in the InSAR data: (1) a northwestward-dipping zone of seismicity and subsidence interpreted as a collapse structure above a mid-crustal magma reservoir and (2) a more diffuse, 8 km-radius zone of shallow seismicity (<2 km), and a largely aseismic zone between 2.5 and 6 km. A second, ∼2 km diameter chamber at 4 km subsurface may underlie the Da'Ure vent, the site of a silicic eruption on 2005 September 26. InSAR and continuous GPS data show uplift above a shallow source in zone (2). The patterns of seismicity provide a working model of magmatic systems maintaining the along-axis segmentation of this incipient seafloor spreading segment. By analogy to the Krafla rifting episode and the rock record in Afar, we have predicted, and seen continued activity in 2006/2007, with a fissural eruption at the southern tip of the segment in 2007 (Yirgu 2007).

ACKNOWLEDGMENTS

This work would have been impossible without the insight and intuition of Laike Mariam Asfaw, Gezahegn Yirgu and Dereje Ayalew. Araya Asfaw, Dean of Sciences at Addis Ababa University, is thanked for his rapid response to the Dabbahu crisis, as is the Ethiopian Air Force for the helicopter support. Feleke Worku, Tesfaye Kidane, Elias Lewi, Negassa, Worku, Julie Rowland, Liz Baker, Juliet Biggs, John Elliott and Addishiwot Woldesenbet were inspirational in the field. Alex Brisbourne and Anna Horleston made extraordinary efforts with the array mobilization and maintenance. Alex Aronovitz assisted with data analyses. Comments by Agust Gudmundsson and anonymous reviewer helped us hone our arguments and improve presentation. This work was supported by NERC grant NE/D008611/1, the Ministry of Capacity Building (Ethiopia), the Afar Government, and NSF grants EAR- 0635789 and EAR-0613651. SAR data were provided by the European Space Agency. TJW acknowledges support from the Royal Society.

REFERENCES

Abdallah, A. *et al.*, 1979. Relevance of Afar seismicity and volcanism to the mechanics of accreting plate boundaries, *Nature,* **282,** 17–23.

Aronovitz, A., Ebinger, C., Campbell, E., Keir, D., Ayele, A. & Mitra, G., 2007. Segment linkage in Afar via magma intrusion: the birth of a transform fault? in *Proceedings of the Eos Trans. Am. Geophys. Union Fall Meeting,* San Francisco, CA.

Ayele, A., Nyblade, A.A., Langston, C.A., Cara, M. & Leveque, J., 2006. New evidence for Afro-Arabian plate separation in southern Afar, in *The Structure and Evolution of the East African Rift System in the Afar Volcanic Province,* Vol. 259, pp. 254–263, eds Yirgu, G., Ebinger, C.J. & Maguire, P.K.H., Special Publication, Geological Society, London.

Ayele, A. *et al.*, 2007a. The volcano-seismic crisis in Afar, Ethiopia, starting September, 2005, *Earth planet. Sci. Lett.,* **255,** 187–197.

Ayele, A., Keir, D., Ebinger, C., Wright, T., Stuart, G., Jacques, E., Ogubazghi, G. & Sholan, J., 2007b. The September 2005 magmato-tectonic activity along the Debbahu-Manda rift basins, A., in *Proceedings of the The Geodynamics of Afar and the Ethiopian Rifts: Geophysics, Geohazard Challenges and Resources Conference (Abstracts)* Addis Ababa University Press, Addis Ababa.

Barberi, F. & Varet, J., 1977. Volcanism of Afar: small-scale plate tectonic implications, *Geol. Soc. Am. Bull.,* **88,** 1251–1266.

Barisin, I., Leprince, S., Avouac, J., Parsons, B. & Wright, T., 2007. Deformation measurements for the September 2005 Afar rifting event from sub-pixel correlation of SPOT images, *Eos, Trans. Am. geophys. Un.* **88**(52), Fall Meeting Suppl., G51C-0633.

Bastow, I., Stuart, G.W., Kendall, J.-M. & Ebinger, C., 2005. Upper mantle seismic structure in a region of incipient continental breakup: northern Ethiopian rift, *Geophys. J. Int.,* **162,** 479–493.

Bendick, B., McClusky, S., Bilham, R., Asfaw, L. & Klemperer, S., 2006. Distributed Nubia-Somalia relative motion and dike intrusion in the Main Ethiopian rift, *Geophys. J. Int.,* doi:10/1111.j.1365-246X.02904.

Benoit, M.H., Nyblade, A.A., VanDecar, J.C. & Gurrola, H., 2003. Upper mantle P wave velocity structure and transition zone thickness beneath the Arabian Shield, *Geophys. Res. Lett.,* **30,** 1531, doi:10.1029/2002GL016436.

Benoit, M. H., Nyblade, A.A. & VanDecar, J.C., 2006. Upper mantle P wave speed variations beneath Ethiopia and the origin of the Afar Hotspot, *Geology,* **34,** 329–332.

Berckhemer, H. *et al.*, 1975. Deep seismic soundings of the Afar region and on the highland of Ethiopia, in *Afar Between Continental and*

Oceanic Rifting, pp. 89–107, eds Pilger, A. and Rosler, A., Schweizerbart, Stuttgart.

Bjornsson, A., Saemundsson, K., Einarsson, P., Tryggvason, E. & Gronvald, K., 1977. Current rifting episode in north Iceland, *Nature,* **266,** 318–323.

Bonafede, M. & Danesi, S., 1997. Near-field modifications of stress induced by dyke injection at shallow depth, *Geophys. J. Int.,* **130,** 435–448.

Brandsdottir, B., Menke, W., Einarsson, P., White, R.S. & Staples, R.K., 1997. Faroe-Iceland Ridge Experiment 2: crustal structure of the Krafla central volcano, *J. geophys. Res.,* **102,** 7867–2886.

Buck, R., Einarsson, P. & Brandsdottir, B., 2007. Tectonic stress and magma chamber size as controls on dike propagation: constraints from the 1975–1984 Krafla rifting episode, *J. geophys. Res.,* **111,** doi:10.1029/2005JB003879.

Casey, M., Ebinger, C., Keir, D., Gloaguen, R. & Mohamed, F., 2006. Extension by dyke extension and faulting in an incipient oceanic rift: Ethiopian rift, Africa, in *The Afar Volcanic Province within the East African Rift System,* Vol. 259, pp. 143–164. eds Yirgu, G., Ebinger, C. and P. Maguire, P., Geol. Soc. London Spec. Pub.

Cattin, R., Doubre, C., de Chabalier, J-B., King, G., Vigny, C., Avouac, J-P. & Ruegg, J-C., 2005. Numerical modelling of Quaternary deformation and post-rifting displacement in the Asal-Ghoubbet rift (Djibouti, Africa), *Earth planet. Sci. Lett.,* **239,** 352–367.

Courtillot, V., Galdeano, A. & Le Mouël, J.-L., 1980. Propagation of an accreting plate boundary: a discussion of new aeromagnetic data in the Gulf of Tadjurah and southern Afar, *Earth planet. Sci. Lett.,* **47,** 144–160.

D'Acremont, E., Leroy, S., Beslier, M-O., Bellahsen, N., Fournier, M., Robin, C., Maia, M. & Gente, P., 2005. Structure and eveolition of the eastern Gulf of Aden margins from seismic reflection data, *Geophys*. *J. Int.,* doi:10.1111/j.1365-246X.2005.02524.

Debayle, E., Lévêque, J.J. & Cara, M., 2001. Seismic evidence for a deeply rooted low velocity anomaly in the upper mantle beneath the northeastern Afro/Arabian continent, *Earth planet. Sci. Lett.,* **193**(3–4), 369–382.

Delaney, J.R., Kelley, D.S., Lilley, M., Butterfield, D.A., Baross, J.A., Wilcock, W.S.D., Embley, R.W. & Summit, M., 1998. The Quantum event of oceanic crustal accretion impacts of diking at mid-ocean ridges, *Science,* **281,** 222–230.

de Zeeuw-van Dalfsen, E., Pedersen, R., Sigmundsson, F. & Pagli, C., 2004. Satellite radar interferometry suggests deep accumulation of magma near the crust-mantle boundary beneath the Krafla volcanic system, Iceland, *Geophys. Res. Lett.,* **31,** doi:10.1029:2004GL020368.

Doubre, C., Manighetti, I., Dorbath, L., Dorbath, C., Jacques, E. & Delmond, J.-C., 2007a. Crustal structure and magmato-tectonic processes in an active rift (Asal-Ghoubbet, Afar, East Africa); 1: insights from a 5-month seismological experiment, *J. geophys. Res.,* **112,** doi:10.1029/2005JB003940.

Doubre, C., Manighetti, I., Dorbath, L., Dorbath, C., Bertil, D. & Delmond, J.-C., 2007b. Crustal structure and magmato-tectonic processes in an active rift (Asal-Ghoubbet, Afar, East Africa); 2: insights from the 23-year recording of seismicity since the last event, *J. geophys. Res.,* **112,** doi:10.1029/2005JB004333.

Dugda, M. & Nyblade, A., 2006. New constraints on crustal structure beneath eastern Afar from analysis of receiver functions and surface wave dispersion in Djibouti, in *Structure and Evolution of the Rift Systems within Afar Volcanic Province, East African Rift,* Vol. 259, eds Yirgu, G., Ebinger, C. and Maguire, P., Geol. Soc. London Spec. Pub.

Dugda, M., Nyblade, A. & Julia, J., 2007. Thin lithosphere beneath Ethiopia and Djibouti revealed by a joint inversion of Rayleigh wave group velocities and receiver functions, *J. geophys. Res.,* **112,** doi:10.1029/2006JB004918.

Eagles, G., Gloaguen, R. & Ebinger, C., 2002. Kinematics of the Danakil microplate, *Earth planet. Sci. Lett.,* **203**(2), 607–620.

Ebinger, C. & Casey, M., 2001. Continental break-up in magmatic provinces: an Ethiopian example, *Geology,* **29,** 527–530.

Einarsson, P., 1991. The Krafla rifting episode 1975–1989, in *Náttúra Myvatns, (The Nature of lake Myvatn),* eds Gardarsson, A. and Einarsson, Á., pp. 97–139, Icelandic Nature Science Society, Reykjavíc.

Einarsson, P. & Brandsdóttir, B., 1980. Seismological evidence for lateral magma intrusion during the July 1978deflation of the Krafla volcano in NE-Iceland, *J. Geophys.,* **47,** 160–165.

Feigl, K.L., Gasperi, F., Sigmundsson, F. & Rigo, A., 2000. Crustal deformation near Hengill volcano, Iceland 1993–1998: coupling between magmatic activity and faulting inferred from elastic modeling of satellite radar interforograms, *J. geophys. Res.,* **105,** 25 655–25 670.

Fialko, Y.A. & Rubin, A.M., 1998. Thermodynamics of lateral dike propagation: Implications for crustal accretion at slow spreading mid-ocean ridges, *J. geophys. Res.,* **103,** 2501–2514.

Foulger, G.R., Jahn, C.-H, Seeber, G., Einarsson, P., Julian, B.R. & Heki, K., 1992. Post rifting stress relaxation at the accretionary plate boundary in Iceland, measured using the Global Positioning System, *Nature,* **358,** 488–490.

Gouin, P., 1979. *Earthquake History of Ethiopia and the Horn of Africa,* International Development Research Centre, Ottawa, Canada, 258 pp.

Grandin, R. *et al.*, 2007, Surface deformation during a magmatic intrusion: the example of the Dabba'hu Rift Crisis of 2005–2006 (Afar, Ethiopia), *Eos, Trans. Am. geophys. Un.,* **88**(Fall Meeting Suppl.), Abstract T51C-0690.

Gresta S., Patanè D., Daniel A., Zan L., Carletti A. & Befekadu O., 1997. Seismological evidences of active faulting in the Tendaho rift (Afar triangle, Ethiopia), *Pure appl. Geophys.,* **149,** 357–374.

Gundmundsson, A., 1995. Infrastructure and mechanics of volcanic systems in Iceland, *J. Volc. Geotherm. Res.,* **64,** 1–22, doi:10.1016/0377-0273(95)92782-Q.

Gudmundsson, A., 2006. How local stresses control magma-chamber ruptures, dyke injections, and eruptions in composite volcanoes, *Earth Sci. Rev.,* **79,** 1–31.

Hayward, N. & Ebinger, C., 1996. Variations in the along-axis segmentation of the Afar rift system, *Tectonics,* **15**(2), 244–257.

Hofstetter, R. & Beyth, M., 2003. The Afar Depression: interpretation of the 1960 2000 earthquakes, *Geophys. J. Int.,* **155,** 715–732.

Jacques, E., Ruegg, J.C., Lépine, J.C., Tapponnier, P., King, G.C.P. & Omar, A., 1999. Relocation of M > 3 events of the 1989 Dobi sequence in Afar: evidence for earthquake migration, *Geophys. J. Int.,* **138,** 447–469.

Keir, D., Ebinger, C.J., Stuart, G.W., Daly, E. & Ayele, A., 2006a. Strain accommodation by magmatism and faulting at continental breakup: Seismicity of the northern Ethiopian rift, *J. geophys. Res.,* **111,** doi:10.1029/2005JB003748.

Keir, D., Stuart, G.W., Jackson, A. & Ayele, A., 2006b. Local earthquake magnitude scale and seismicity rate for the Ethiopian rift, *Bull. seism. Soc. Am.,* **96,** doi:10.1785/0120060051.

Keir, D. *et al.*, 2008. Repeated dike injection sourced beneath the center of the Dabbahu segment in the Afar rift, *Geology,* submitted.

Kidane, T. *et al.*, 2003. New Paleomagnetic and geochronological results from Ethiopian Afar: block rotations linked to rift overlap and propagation and determination of a similar to 2 Ma reference pole for stable Africa, *J. geophys. Res.,* **108,** doi:2102:00018198520001.

Klein, F.W., 2002. User's guide to Hypoinverse-2000, a FORTRAN program to solve for earthquake locations and magnitudes, U.S. Geol. Surv. Open File Rep., 02-171, pp. 1–123.

Lahitte, P., Gillot, P.-Y., Kidane, T., Courtillot, V. & Abebe, B., 2003. New age constraints on the timing of volcanism in central Afar, in the presence of propagating rifts, *J. geophys. Res.,* **108,** doi:10.1029/2001JB001689.

Macdonald, K.C., 1998. Linkages between faulting, volcanism, hydrothermal activity and segmentation on fast-spreading centers, in *Faulting and Magmatism at Mid-Ocean Ridges,* Vol. 106, Geophysical Monograph, 348 p., eds Buck, W.R., Karson, J.A. and Lagabrielle, Y., pp. 27–59, American Geophysical Union, Washington DC.

Manighetti, I., Tapponnier, P., Courtillot, V., Gruszow, S. & Gillot, P-Y., 1997. Propagation of rifting along the Arabia-Somalia plate boundary: the gulfs of Aden and Tadjoura, *J. geophys. Res.,* **102,** 2681–2710.

Oppenheimer, C. & Francis, P., 1998. Implications of longeval lava lakes for geomorphological and plutonic processes at Erta 'Ale volcano, north Afar, *J. Volc. Geoth. Res.,* **80,** 101–111.

Préjean, S., Stork, A., Ellsworth, W., Hill, D. & Julian, B., 2003. High precision earthquake locations reveal seismogenic structure beneath Mammoth Mountain, California, *Geophys. Res., Lett.,* **30,** doi:1029/2003GL018334.

Roman, D.C. & Heron, P., 2007. Effect of regional tectonic setting on local fault response to episodes of volcanic activity, *Geophys. Res. Lett.,* **34,** doi:10.1029/2007GL030222.

Rowland, J.R., Baker, E., Ebinger, C., Keir, D., Kidane, T., Biggs, J., Hayward, N. & Wright, T., 2007. Fault growth at a nascent slow-spreading ridge: 2005 Dabbahu rifting episode, Afar, *Geophys. J. Int.,* **171,** doi:1111/j.1365-246X.2007.03584.x.

Rubin, A., 1992. Dike-induced faulting and graben subsidence in volcanic rift zones, *J. geophys. Res.,* **97,** 1839–1858.

Rubin, A. & Gillard, D., 1998. Dike-induced earthquakes: theoretical considerations, *J. geophys. Res.,* **103,** 10 017–10 030.

Rubin, A. & Pollard, D., 1988. Dike-induced faulting in rift zones in Iceland and Afar, *Geology,* **16,** 413–417.

Rubin, A., Gillard, D. & Got, J-L., 1998. Re-interpretation of seismicity associated with the January 1983dike intrusion at Kilauea volcano, Hawaii, *J. geophys. Res.,* **103,** 10 003–10 015.

Ruegg, J.-C., 1975. Structure profonde de la croute et du manteau superieur du Sud-Est de l'Afar d'après les données sismiques, *Ann. Geophys.,* **31,** 329–360.

Sigmundsson, F., 1992. Tectonic implications of the 1989 Afar earthquake sequence, *Geophys. Res. Lett.,* **19,** 877–880.

Sigmundsson, F., 2006. *Iceland Geodynamics: Crustal Deformation and Divergent Plate Tectonics,* Springer-Praxis, Chichester, UK, 228p.

Snoke, J.A., 2003. FOCMEC: focal mechanism determinations (Chapter 85.12), in *International Handbook of Earthquake and Engineering Seismology,* eds Lee, W.H.K., Kanamori, H., Jennings, P.C. and Kisslinger, C., Academic Press, San Diego.

Souriot, Th. & Brun, J-P., 1992. Faulting and block rotation in the Afar triangle, Africa; the Danakil crank-arm model, *Geology,* **20,** 911–914.

Stuart, G., Bastow, I. & Ebinger, C., 2006. Crustal structure of the Northern Main Ethiopian Rift from receiver function studies, in *Structure and Evolution of the Rift Systems within Afar volcanic province, East African rift,* Vol. 259, pp. 253–268. eds Yirgu, G., Ebinger, C., and Maguire, P., Geol. Soc. London Spec. Pub.

Tryggvason, E., 1994. Surface deformation at the Krafla volcano, North Iceland, 1982–1992, *Bull. Volcanol.,* **56,** 98–107.

Vigny, C., DeChabalier, J.B., Ruegg, J.C., Huchon, P., Feigl, K., Cattin, R., Asfaw, L. & Khanbari, K., 2006. 25 years of geodetic measurements along the Tadjoura-Asal rift system, Djibouti, East Africa, *J. geophys. Res.,* **111,** doi:10.1029/2004JB003230.

Waldhauser, F. & Ellsworth, W., 2000. A double-difference earthquake location algorithm: method and application to the northern Hayward fault, California, *Bull. seism. Soc. Am.,* **90,** 1353–1368.

Whitehead, J., Dick, H.J.B. & Schouten, H., 1984. A mechanism for magmatic accretion under spreading centres, *Nature,* **312,** 146–148.

Wolfenden, E., Ebinger, C., Yirgu, G., Renne, P. & Kelley, S.P., 2005. Evolution of the southern Red Sea rift: birth of a magmatic margin, *Geol. Soc. Amer. Bull.,* **117,** 846–864.

Wright, T., Ebinger, C., Biggs, J., Ayele, A., Yirgu, G., Keir, D. & Stork, A., 2006. Magma-maintained rift segmentation at continental rupture in the 2005 Afar dyking episode, *Nature,* **442,** doi:10.1038/nature04978.

Yirgu, G., Ayele, A. & Ayalew, D., 2006. Recent seismo-volcanic crisis in northern Afar, Ethiopia, *Eos, Trans. Am. geophys. Un.,* **87,** 325–336.

Yirgu, G., 2007. The August 2007fissure eruption on the Dabbahu rift segment, *in Proceedings of the Active Volcanism and Continental Rifting Conference: 26th ECGS Workshop,* Luxembourg, 2007 November.